

## Original Research Article

# **Numerical modeling of the effect of the ratio of thermal conductivity on the thin film condensation in forced convection in a canal whose walls are covered with a porous material**

**Abstract** – A numerical modeling of the effect of the ratio of thermal conductivity on the thin film condensation in forced convection in a canal whose walls are covered with a porous material is presented. In this work, the generalized Darcy-Brinkman-Forchheimer (DBF) equations in the porous medium and the hydrodynamic and thermal boundary layer equations in the pure liquid, were used.

Rendered dimensionless and homotopically transformed into a new rectangular basis, we used a finite difference method to discretize them. The advection and the diffusion terms are discretized with respectively a backward-centered scheme and a centered scheme.

After validation, we find that a variation of the longitudinal velocity as a function of the ratio of thermal conductivity only for low values of the Peclet number. When the ratio of thermal conductivity increases, corresponding to an increasingly conductive medium, the longitudinal velocity, the temperature and the Nusselt number increase (even when the Peclet number is high for the thermal field). While the thickness of the liquid film decreases (disadvantaged condensation) and leads to an increase in the length of entry, increase almost linear. The sensitivity of condensation to variations in the ratio of thermal conductivity is constant, whatever its value.

The ratio of thermal conductivity is a very decisive and predictable physical quantity to properly examine the performance of condensation.

**Keywords:** Channel with Porous Wall, Condensation Thin Film, Generalized Darcy-Brinkman- Forchheimer Model, iterative Gauss-Seidel relaxation method, Lengths of Entry, ratio of thermal conductivity

## **1. Introduction**

Implemented in many technological fields such as distillation, heat exchangers, energy storage, cooling of electronic components, drying, desalination, distillation ..., heat and mass transfer during condensation saturated steam in porous media have received considerable attention in many theoretical and experimental studies [1-20].

Shekarriz and Plumb [1] have shown that the presence of porous medium on the condensation of the film on the external wall of a horizontal tube contributes to significantly reduce the thickness of the liquid film and therefore improves the heat exchange with the wall. Chaynane R. and al. [2] investigated the effects of effective viscosity, permeability, and dimensionless thickness of the porous coating on flow and heat transfer refinement. With analytical and numerical studies of a vapor thin film condensation problem in a porous medium Asbik M and al. [3] compared the Darcy-Brinkman (DB) model and the Darcy-Brinkman-Forchheimer (DBF) model. They showed in their results the influences of the Reynolds and Darcy numbers and the dimensionless thickness of the porous layer on the velocity and temperature profiles

in the porous layer, the liquid film thickness, the local Nusselt number. By producing a numerical model of the condensation of pure saturated vapor of the thin film type in forced convection on a wall covered with porous material, Ndiaye M. and al. [4-7] exposed the influences of the thermal conductivity ratio, of the Froude, Reynolds, Prandtl, and Jacob numbers, of the dimensionless thickness of the porous layer and on the transfers in the porous medium and in the liquid phase. Patil A. A. and al. [8] showed that the daily distillate production increases up to 43% by coupling the surface condenser and vacuum pump due to the increase in evaporation and condensation rate by presenting a distillation system of solar water with a combination of surface condenser and vacuum pump. By proposing a numerical study A. Nasr and S. Al-Ghamdi [10] confirmed that the presence of the porous layer improves the performance of heat and mass transfer at the liquid-gas interface during the evaporation of the film liquid in free convection. Abdelaziz Nasr [11] showed numerically that the performance of heat and mass transfer at the liquid-gas interface during the condensation of the liquid film is improved by the presence of the porous layer by studying a numerical model of improvement of the liquid heat and mass transfer film condensation by covering a porous layer on one of the vertical channel plates. Charef A. and al. [12] presented a numerical study of liquid film condensation from vapour-gas mixtures of HFC refrigerants inside a vertical tube and concluded that the condensation of R152a-air corresponds to accumulated condensation  $m_{cd}$  and a higher local heat transfer coefficient  $h_T$  compared to R134a-air under the same conditions. Mosaad M. E-S. and al. [13] presented a model of a regular process of condensation of a laminar film on a vertical wall with the rear face cooled by free convection in a porous medium saturated with fluid. They found a difference compared to the Nusselt type solution (absence of the porous medium). In a thermal desalination process, which is based on the phase change phenomenon, Charef A. and al. [14] proposed a model on liquid film condensation and showed that increasing the temperature difference between the inlet and the wall improves condensation (and therefore the thickness of the condensate film), the radius of the tube and non-condensable gas are also relevant factors to improve the efficiency of thermal desalination. Sellami K. and al [15] found that the evaporative cooler is more efficient for high porosity and thick porous media, with up to 23% improvement for high porosity. Ndiaye P.T. and al. [16-18] presented numerical models of thin film type condensation in forced convection of pure saturated steam in a channel whose walls are covered with a porous material. They studied the influence of the Reynolds, Prandtl and Jacob numbers, the aspect ratio on the longitudinal velocity and the temperature, the heat transfer rate at the interface of the porous medium and the liquid film (Nusselt number local) and on condensation and its sensitivity via liquid film thickness and length of entry. Ndiaye G. and al. [19-20] proposing on numerical studies of the condensation in forced convection of a laminar film of a pure and saturated vapor on a porous plate inclined towards the vertical, examined the effects of different parameters such as: the inclination, effective viscosity and dimensionless thermal conductivity, Reynolds and Prandtl numbers on flow and heat transfer.

In this work, we want to numerically study the effect of the ratio of thermal conductivity on the heat transfer and on the performance of the condensation. To properly carry out this project, we will first proceed to the mathematical formulation with the descriptions of the simplifying hypotheses, the equations of the problem and the boundary conditions. The hydrodynamic and thermal equations of the boundary layer will be used in the pure liquid and the generalized Darcy-Brinkman-Forchheimer (DBF) equations in the porous medium. Then announce the numerical resolution method and finally evaluate the influence of the ratio of

thermal conductivity on the velocity and temperature profiles in porous medium and pure liquid, the thickness of the liquid film, the local Nusselt number (the transfer rate of heat) and lengths of entry (which characterizes condensation).

## 2. Mathematical formulation:

### 2.1 Physical model and assumptions :

We present the modeling of flows and transfers during thin film vapor condensation in porous media. To investigate this resulting condensation phenomenon, we consider the physical model (channel) and coordinate system shown in Figure 1.

This channel is formed by two flat plates, vertical and parallel, the internal walls of which are covered with a porous material of permeability  $K$  and porosity  $\varepsilon$ , of thickness  $H$ . These plates are spaced apart by a distance  $2A$ , of length  $L$  and are maintained at a temperature  $T_w$  lower than that of a saturated vapor  $T_s$  which flows at a uniform speed  $U_0$  at the channel inlet.

This shows the condensation of pure vapor on the porous medium and the presence of three zones: (1) the porous medium saturated with the liquid (2) the film of condensate (3) pure saturated vapor. The condensate film flows under the effect of the forces of gravity and viscous friction. The Cartesian coordinates  $(x, y)$  and the velocity components  $(u, v)$  in the porous medium and the pure liquid in the frame are associated with the model (channel).

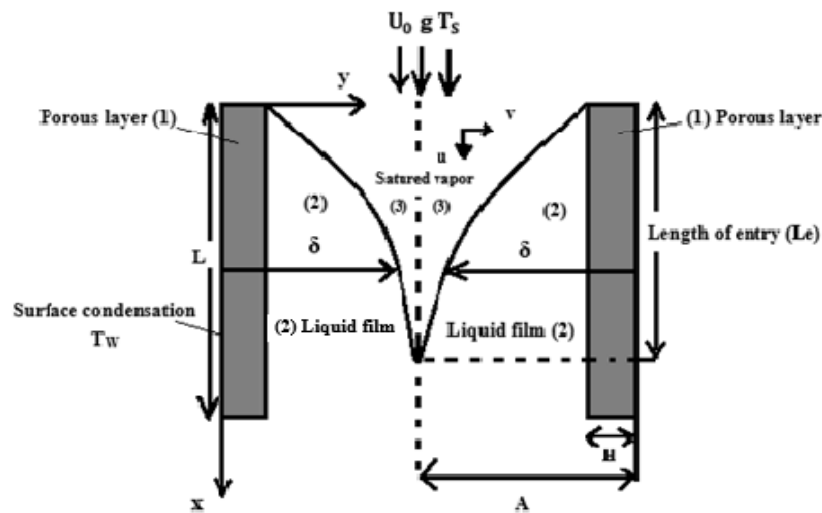


Fig 1 Geometry of the physical model and coordinate system

In order to achieve a coherent mathematical modeling of the physical problem and to reason the difficulties related to the resolution of the governing equations of the phenomenon, we considered the following simplifying hypotheses:

- 1-The hydrodynamic and thermal boundary layer approximations are valid.
- 2--The matrix or porous material is isotropic and homogeneous.
- 3-The porous medium is saturated with a fluid (pure saturated vapor) supposed Newtonian and incompressible (where the equations of the flow and transfer in the vapor phase (3) are generally neglected).

- 4-The generated flow is permanent, laminar and two-dimensional
- 5-The working, induced by the viscous and pressure forces, is negligible.
- 6-The thermo-physical properties of the fluids and the ones of the porous matrix are assumed to be constant in the studied temperature range (the imposed temperature variations do not modify the thermo-physical properties of the fluid which remain constant).
- 7-The generalized model of Darcy-Brinkman-Forchheimer (DBF) is used to describe the flow in the porous layer.
8. Condensation occurs in the form of a thin film of greater thickness than the porous material
- 9-The porous matrix is in local equilibrium with the condensate.
- 10-The liquid-vapor interface is in thermodynamic equilibrium.
- 11- The solid and the fluid phases of the porous medium are in thermal equilibrium
- 12-The transverse and the longitudinal variation of the pressure is not taken into account in the porous matrix.
- 13-The transfer of energy by radiation is neglected
- 14-The geometry of the problem makes the flow considered axisymmetric.

## 2.2 Dimensionless Equations, Determination of local Nusselt number and length of entry

In the domains (1) and (2) already defined, the equations which govern the transfers and the boundary conditions associated with them have been made dimensionless by using the following variables and parameters. We pose:

$$x^* = \frac{x}{L} \quad (1) \quad ; \quad y^* = \frac{y}{A} \quad (2) \quad ; \quad H^* = \frac{H}{A} \quad (3) \quad ; \quad \delta^* = \frac{\delta}{A} \quad (4) \quad ; \quad u^* = \frac{u}{U_0} \quad (5)$$

$$v^* = \frac{v}{U_0} \quad (6) \quad ; \quad \theta = \frac{T - T_w}{T_s - T_w} \quad (7) \quad ; \quad \lambda^* = \frac{\lambda_l}{\lambda_{eff}} \quad (8) \quad ; \quad v^* = \frac{v_{eff}}{v_l} \quad (9)$$

The dimensionless physical domain  $(x^*, y^*)$  thus obtained presents a curvilinear interface (liquid/pure vapor interface), we will transform it into a rectangular domain  $(\mathbf{X}, \boldsymbol{\eta})$  in which the boundary and the interfaces (porous medium interfaces /pure liquid and pure liquid/vapour) will be identified by lines of constant coordinates. The following change (homotopic transformation) of variable is made:

$$\begin{cases} X = x^* \\ \eta = coef \cdot \frac{y^*}{H^*} + (1 - coef) \left\{ 1 + \frac{y^* - H^*}{\delta^*(X) - H^*} \right\} \end{cases} \quad (10)$$

With *Coef* it is a coefficient equal to 1 in the porous layer and 0 in the pure liquid. Thus the frame  $(x^*, y^*)$  is transformed into a rectangular field  $(\mathbf{X}, \boldsymbol{\eta})$ . The porous medium / pure liquid interface is parametrized by the straight line with coordinate  $\eta = 1$  and the pure liquid / vapor interface is parametrized by the straight line with coordinate  $\eta = 2$ .

In both media, the dimensionless equations in the rectangular domain  $(\mathbf{X}, \boldsymbol{\eta})$  are written:

**Porous layer:**  $0 \leq \eta \leq 1$

The equation of conservation of mass or equation of continuity is:

$$\frac{\partial u_p^*}{\partial X} + \frac{L}{A} \frac{1}{H^*} \frac{\partial v_p^*}{\partial \eta} = 0 \quad (11)$$

The equation of momentum following X-direction is:

$$u_p^* \frac{\partial u_p^*}{\partial X} + \frac{L}{A} \frac{v_p^*}{H^*} \frac{\partial u_p^*}{\partial \eta} = \frac{\varepsilon^2}{Fr} - \varepsilon^2 \left( \frac{L}{A} \right)^2 \frac{v^* . Da}{Re} u_p^* + \varepsilon^2 \left( \frac{L}{A} \right)^2 v^* \frac{1}{Re H^{*2}} \frac{\partial^2 u_p^*}{\partial \eta^2} - \varepsilon^2 F \sqrt{Da} \frac{L}{A} u_p^{*2} \quad (12)$$

The equation of heat is:

$$u_p^* \frac{\partial \theta_p}{\partial X} + \frac{L}{A} \frac{v_p^*}{H^*} \frac{\partial \theta_p}{\partial \eta} = \left( \frac{L}{A} \right)^2 \frac{1}{Re Pr_{eff} H^{*2}} \frac{\partial^2 \theta_p}{\partial \eta^2} \quad (13)$$

**Pure liquid:**  $1 \leq \eta \leq 2$

The equation of conservation of mass or equation of continuity is:

$$\frac{\partial u_l^*}{\partial X} - \frac{(\eta-1)}{(\delta^*(X)-H^*)} \frac{d\delta^*(X)}{dX} \frac{\partial u_l^*}{\partial \eta} + \frac{L}{A} \frac{1}{(\delta^*(X)-H^*)} \frac{\partial v_l^*}{\partial \eta} = 0 \quad (14)$$

The equation of momentum following X-direction is:

$$u_l^* \left[ \frac{\partial u_l^*}{\partial X} - \frac{\eta-1}{\delta^*(X)-H^*} \frac{d\delta^*(X)}{dX} \frac{\partial u_l^*}{\partial \eta} \right] + \frac{L}{A} \frac{v_l^*}{\delta^*(X)-H^*} \frac{\partial u_l^*}{\partial \eta} = \left( \frac{L}{A} \right)^2 \frac{1}{Re (\delta^*(X)-H^*)^2} \frac{\partial^2 u_l^*}{\partial \eta^2} + \frac{1}{Fr} \left( 1 - \frac{\rho_v}{\rho_l} \right) \quad (15)$$

The equation of heat is:

$$u_l^* \left[ \frac{\partial \theta_l}{\partial X} - \frac{\eta-1}{\delta^*(X)-H^*} \frac{d\delta^*(X)}{dX} \frac{\partial \theta_l}{\partial \eta} \right] + \frac{L}{A} \frac{v_l^*}{\delta^*(X)-H^*} \frac{\partial \theta_l}{\partial \eta} = \left( \frac{L}{A} \right)^2 \frac{1}{Re Pr (\delta^*(X)-H^*)^2} \frac{\partial^2 \theta_l}{\partial \eta^2} \quad (16)$$

To these equations are added the following boundary and dimensionless continuity conditions:

Conditions at the entry:  $X=0$

$$u_p^*(0, \eta) = 1 \quad (17) \quad ; \quad v_p^*(0, \eta) = 0 \quad (18) \quad ; \quad \theta_p(0, \eta) = 1 \quad (19)$$

Boundary conditions at the wall:  $\eta = 0$

$$u_p^* = v_p^* = 0 \quad (20) \quad ; \quad \theta_p = 0 \quad (21) \quad ; \quad u_p^* = v_p^* = 0 \quad (22) \quad ; \quad \theta_p = 0 \quad (23)$$

At the porous/pure liquid interface:  $\eta = 1$

$$u_l^* = u_p^* \quad (24) \quad ; \quad \theta_l = \theta_p \quad (25)$$

Continuity of constraints

$$\frac{\mu^*}{H^*} \frac{\partial u_p^*}{\partial \eta} = \frac{1}{(\delta^*(X)-H^*)} \frac{\partial u_l^*}{\partial \eta} \quad (26)$$

Continuity of thermal flows:

$$\frac{1}{H^*} \frac{\partial \theta_p}{\partial \eta} = \frac{\lambda^*}{(\delta^*(X) - H^*)} \frac{\partial \theta_l}{\partial \eta} \quad (27)$$

At the liquid / vapor interface  $\eta = 2$

$$\theta_l = 1 \quad (28) ; \quad \frac{\partial u_l^*}{\partial \eta} = 0 \quad (29)$$

The dimensionless speed and temperature depending on the thickness of the liquid film, the heat and mass balances can be coupled. The coupled equation of mass flow and heat balance made dimensionless is expressed by the following relationship:

$$\left(\frac{L}{A}\right)^2 \frac{Ja}{(Pe)_{eff}} \frac{1}{H^*} \frac{\partial \theta_p}{\partial \eta} /_{\eta=0} = \frac{d}{dX} \left\{ (1+Ja)\delta^*(X) \frac{\rho_v}{\rho_l} \right\} - Ja \frac{d}{dX} \left\{ H^* \int_0^1 \theta_p u_p^* d\eta + (\delta^*(X) - H^*) \int_1^2 \theta_l u_l^* d\eta \right\} \quad (30)$$

With:

The mass flow rate:

$$H^* \int_0^1 u_p^* d\eta + (\delta^*(X) - H^*) \int_1^2 u_l^* d\eta = \frac{\rho_v \delta^*(X)}{\rho_l} \quad (31)$$

Number of Jacob:

$$Ja = \frac{Cp_l (T_s - T_w)}{h_{fg}} \quad (32)$$

Number of Froude:

$$Fr = \frac{U_0^2}{gL} \quad (33)$$

Number of Reynolds:

$$Re = \frac{U_0 L}{\nu_l} = v^* \frac{U_0 L}{\nu_{eff}} \quad (34)$$

Number of Darcy:

$$Da = \frac{A^2}{K} \quad (35)$$

Number of Prandtl:

$$Pr = \frac{\nu_l}{\alpha_l} = \frac{\mu_l C_{pl}}{\lambda_l} \quad (36)$$

Number of Peclet:

$$Pe = Re \cdot Pr \quad (37)$$

Number of Peclet modified:

$$Pe_{eff} = \lambda^* Pe = \lambda^* Re \cdot Pr \quad (38)$$

Number of de Prandtl modified:

$$Pr_{eff} = \lambda^* Pr \quad (39)$$

## Determination of local Nusselt number

The **local Nusselt number** is the gradient in temperature at the interface porous medium and liquid film.

$$Nu = \frac{1}{\delta^*(X) - H} \left. \frac{\partial \theta_l}{\partial \eta} \right]_{\eta=1} \quad (40)$$

### Determination of the Lengths of Entry (Le)

Already defined by Ndiaye P. T. and al. [16-18], the length of entry (Le) is a length from the channel inlet to the meeting of the two liquid films.

It is the length on the channel beyond which the boundaries layers conditions are not applicable any more

$$\delta(x = Le) = A \quad (41)$$

In dimensionless form and a rectangular domain, it is:

$$\delta^*(X = Le^*) = 1 \quad (42)$$

The partial differential equations which govern our problem are not only nonlinear, coupled between them, also coupled with their boundary conditions. They generally do not have analytical solutions, except for very simplified cases. A numerical resolution is essential for not simplified cases and thus for ours.

## 3. Numerical methodology

It comprises two parts: a mesh part and a discretization part. We considered the mesh of the numerical domain uniform in the longitudinal and transverse directions and for the discretization an implicit finite difference method. The advection terms are discretized respectively with a backward off-center scheme. The terms and diffusion are discretized with a centered scheme. This will make possible the main diagonals of the most dominant matrices possible (for more stability). The systems of coupled algebraic equations thus obtained will be solved numerically thanks to a double sweep method combined with an iterative scheme of sub-relaxation line by line of the Gauss-Seidel type, in general faster than several other algorithms (such as the Jacobi's algorithm). Under-relaxation coefficients have been empirically defined to guarantee the non-growth of calculation errors during the iterative process. This will make our patterns or system more stable and convergent. All the results from the numerical simulation were obtained from a FORTRAN code.

## 4. Results and discussion

### 4.1 Results of method validation:

The results of our calculation model have been validated in comparison with the work of Ndiaye M. (2014). Since his model is only valid for values of the Reynolds number lower than 7, we made the comparison by taking low Reynolds numbers ( $Re=2$ ) and low permeability (high Darcy number,  $Da=10^{12}$ ). We took  $\Delta X = 0.0001$  and  $\Delta \eta = 0.02$ , for the study of the sensitivity of the mesh in order to answer at the same time to the speed, the precision and the convergence of the calculations.

We have a good concordance with Ndiaye M. and al. [4-7], which will allow us to validate our model.

## 4.2 Results and discussions

In this study, we show the effect of the ratio of thermal conductivity on the longitudinal velocity, the temperature, the film thickness, the thermal transfer rate at the porous medium/liquid film interface (local Nusselt number) and finally along the length of entry. We remind that the ratio of thermal conductivity is the ratio of the thermal conductivity of the liquid film on the thermal conductivity of the porous material.

The results from the numerical simulations are related to:

$$\varepsilon = 0.4; F = 0.55; v^* = 1; Da = 10^9; Fr = 10^{-4}$$

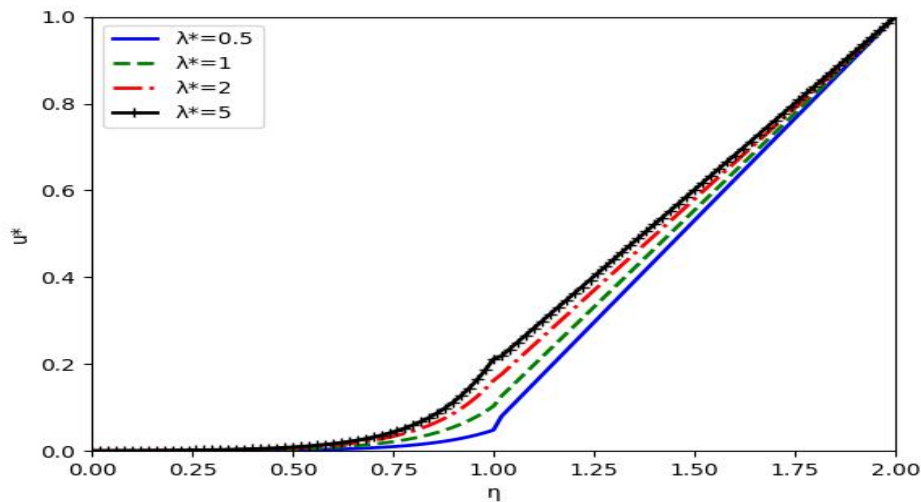


Figure 2 : Variation de la vitesse longitudinale en fonction de l'ordonnée  $\eta$  pour différentes valeurs de  $\lambda^*$  à la position  $X=0.05$

$$Re=25; Fr=10^{-4}; Pr=1; H^*=2.10^{-4}; Ja=10^{-8}; v^*=1; Da=10^9; L/A=10$$

The curve in Figure 2 shows that when the ratio of thermal conductivity increases, the longitudinal velocity increases ( $Re = 10; Pr = 1$ ) and for Figure 3 the variations in the ratio of thermal conductivity are accompanied by a small variation in the longitudinal velocity ( $Re = 50; Pr = 7$ ). In general we have a variation of the longitudinal velocity as a function of the thermal conductivity ratio only for low values of the Peclet number ( $Pe = Re.Pr$ ). The flow is characterized by the Peclet number which indicates the relative importance of convection and diffusion (thermal conduction), diffusion is strongly dominant when the Peclet number is low (Fig. 2,  $Pe=10$ ). When it is high (Fig. 3,  $Pe=350$ ) convection is strongly dominant and the velocity is not influenced by the variation of the ratio of thermal conductivity.

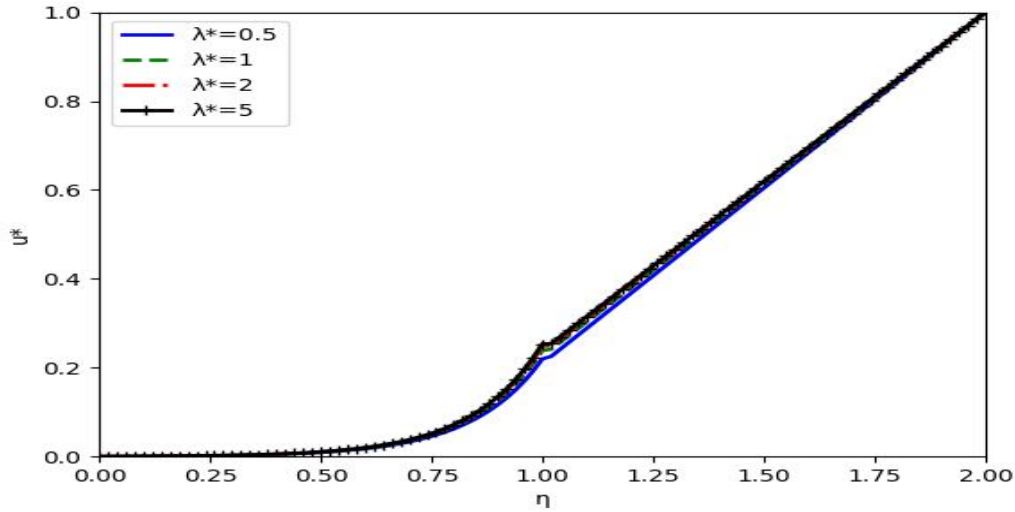


Figure 3 : Variation de la vitesse longitudinale en fonction de l'ordonnée  $\eta$  pour différentes valeurs de  $\lambda^*$  à la position  $X=0.05$

$$Re=50 ; Fr=10^{-4} ; Pr=7 ; H^*=2.10^{-4} ; Ja=10^{-8} ; v^*=1 ; Da=10^9 ; L/A=10$$

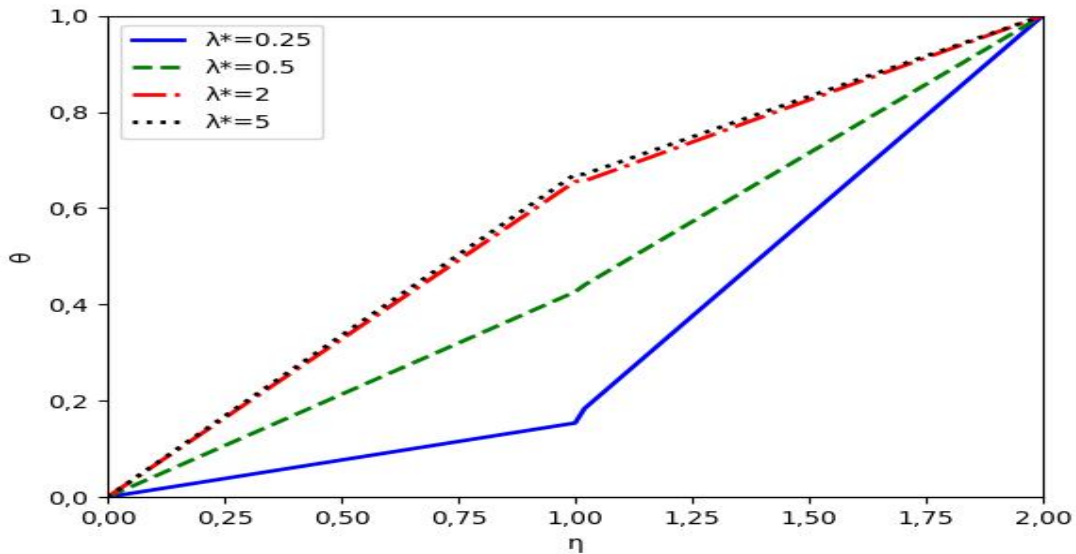
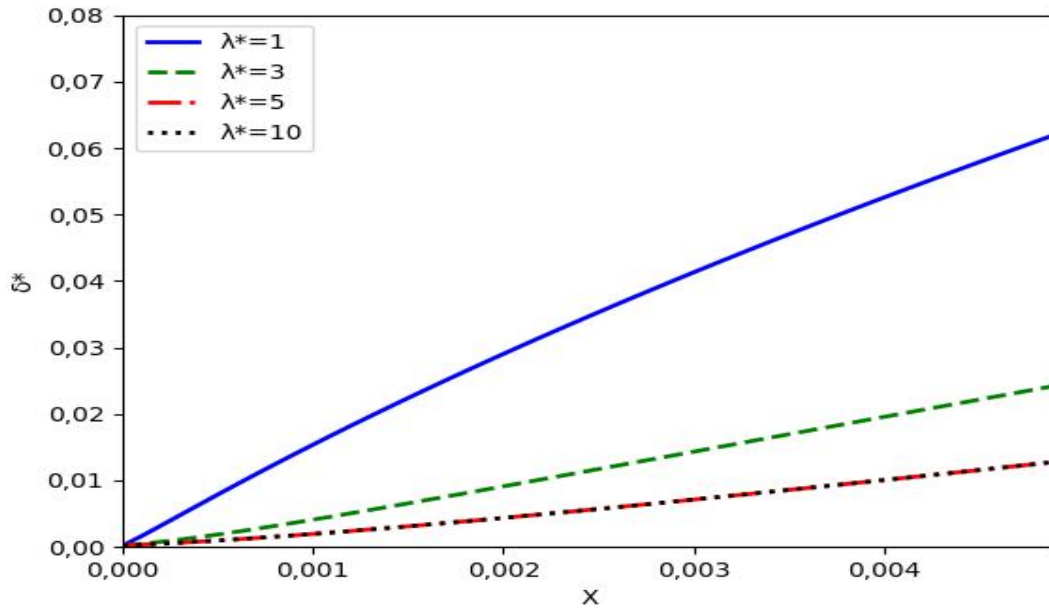


Figure 4 : Variation de la température longitudinale en fonction de l'ordonnée  $\eta$  pour différentes valeurs de  $\lambda^*$

$$Re=100 ; Fr=10^{-4} ; Pr=5 ; H^*=2.10^{-4} ; Ja=10^{-8} ; v^*=1 ; Da=10^9 ; L/A=100$$

For Figure 4 when the ratio of thermal conductivity increases, the temperature increases even when the Peclet number is high ( $Pe=500$ ). The thickness of the liquid film being much greater than that of the porous material, hence the conductive transfers in the liquid film are much more dominant, most of the transfers take place in the liquid film. Large values of the thermal conductivity ratio correspond to a highly conductive liquid phase.



**Figure 5: Variation de l'épaisseur du film liquide en fonction de l'abscisse X pour différentes valeurs  $\lambda^*$**

$$Re=100 ; Fr=10^{-4} ; Pr=5 ; H^*=2.10^{-4} ; Ja=10^{-8} ; v^*=1 ; Da=10^9 ; L/A=100$$

With Figure 5 we found that the dimensionless thickness of the liquid film decreases when the ratio of thermal conductivity increases (Figure 5). By reducing the thermal conductivity of the liquid film compared to that of the porous material, the transfer and the heat exchange (conductive) are lowered, which allows better contact with the cold plate and condensation is favored.

We study the variation of the Nusselt number, heat transfer rate at the porous medium/pure liquid interface and the ratio between convective heat transfer and conductive transfer as a function of the abscissa X (Figure 6). At the entrance to the channel, the value of the Nusselt number is very high, then rapidly decreases along the porous wall to reach very low asymptotic values. Conduction gradually increases along the porous wall on convective heat transfer. This justifies the decrease in the Nusselt number as a function of the abscissa X. We note the increase in the ratio of thermal conductivity (increase in the thermal conductivity of the liquid film compared to that of the porous material) leads to an increase in the Nusselt number (Figure 6), even when the Peclet number is high ( $Pe=125$ ). Their growth is consistent with an increasingly conductive environment. (This increases the heat exchanges at the interface between the porous medium and the pure liquid.)

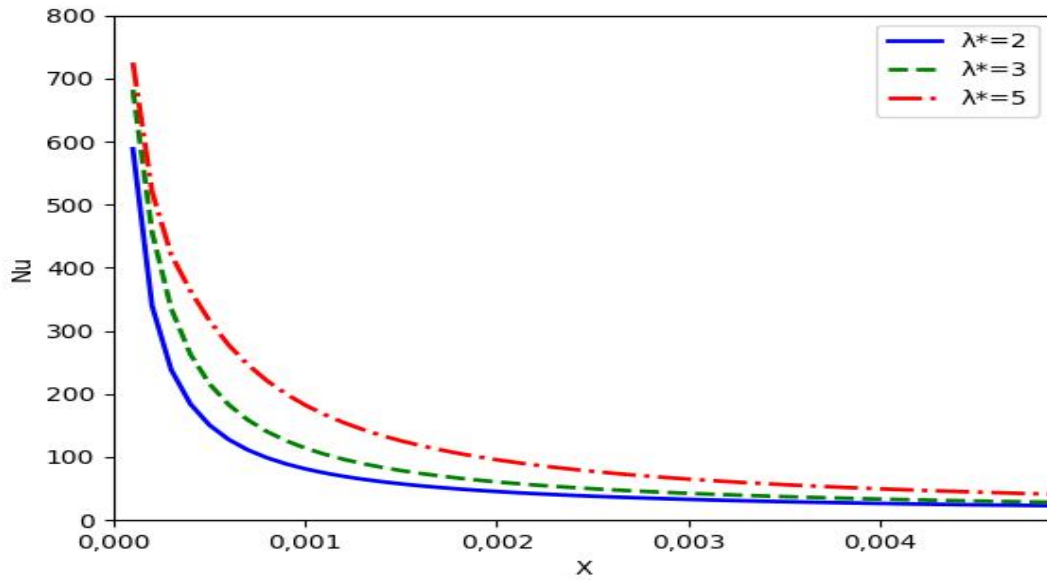


**Figure 6** Variation du nombre de Nusselt en fonction de l'abscisse X pour différentes valeurs de  $\lambda^*$

$$Re=25 ; Fr=10^{-4} ; Pr=5 ; H^*=2.10^{-4} ; Ja=10^{-8} ; \nu^*=1 ; Da=10^9 ; L/A=100$$

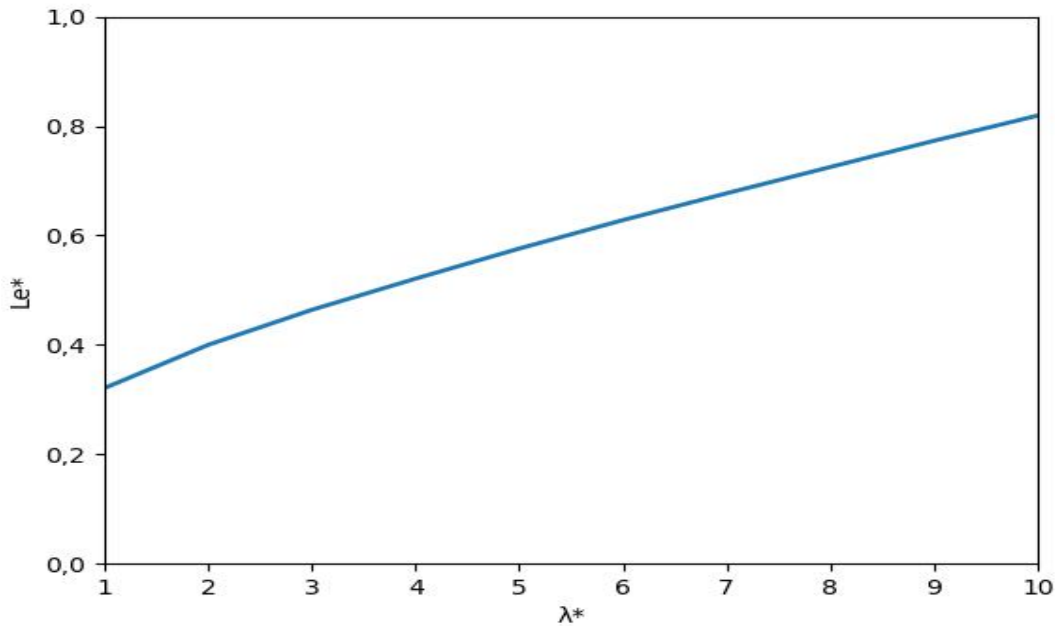


**Figure 7:** variation de la longueur d'entrée adimensionnelle ( $Le^*$ ) en fonction de  $\lambda^*$

$$Re=50 ; Fr=10^{-4} ; Pr=5 ; H^*=2.10^{-4} ; Ja=10^{-8} ; \nu^*=1 ; Da=10^9 ; L/A=100$$

Figure 7 is the variation of the dimensionless length of entry as a function of the ratio of thermal conductivity (increase in the thermal conductivity of the liquid film compared to that of the porous material). It provides information on the sensitivity of the condensation to the

variation of the ratio of thermal conductivity. The variations of the dimensionless length of entry (Figure 7) confirm those of the dimensionless thickness of the liquid film (Fig. 5).

A reduction thickness of liquid film produces an increase length of entry. From where the variations in the dimensionless length of entry (Figure 7) confirm those the dimensionless thickness of liquid film (Figure 5), i.e. the increase in the ratio of thermal conductivity decrease the thickness of liquid film and increase the length of entry. This increase of length of entry is almost linear. The sensitivity of condensation to variations in the ratio of thermal conductivity is constant, whatever its value. The ratio of thermal conductivity is a very decisive physical parameter to properly examine the performance of condensation.

## 5. Conclusion

We have proposed a numerical modeling of the effect of the ratio of thermal conductivity on the thin film condensation in forced convection in a canal whose walls are covered with a porous material.

Using the generalized Darcy-Brinkman-Forchheimer (DBF) equations in the porous medium and the hydrodynamic and thermal boundary layer equations in the pure liquid, we used a finite difference method to discretize the latter rendered dimensionless, homotopically transformed into a new rectangular base. The advection and the diffusion terms are discretized with respectively a backward-centered scheme and a centered scheme. Our results, compared to those of Ndiaye M. and al. [4-7] have been validated.

We analyzed the influence of the ratio of thermal conductivity on the longitudinal velocity, the temperature, the film thickness, the thermal transfer rate at the porous medium/liquid film interface (local Nusselt number) and finally on the length of entry. We have a variation of the longitudinal velocity as a function of the ratio of thermal conductivity only for low values of the Peclet number. When the ratio of thermal conductivity increases, corresponding to an increasingly conductive medium, the longitudinal velocity, the temperature and the Nusselt number increase (even when the Peclet number is high for the temperature and the Nusselt number, so the thermal field). While the thickness of the liquid film decreases (disadvantaged condensation) and leads to an increase in the length of entry. This increase in the length of entry as a function of the ratio of thermal conductivity is almost linear. The sensitivity of condensation to variations in the ratio of thermal conductivity is constant, whatever its value. The ratio of thermal conductivity is a very decisive and predictable physical quantity to properly examine the performance of condensation.

## Nomenclature

### Greeks symbols

$\alpha$ : thermal diffusivity,  $m^2.s^{-1}$

$\delta$  thickness of condensate, m

$\varepsilon$  : Porosity

$\eta$  : dimensionless coordinate in the transverse direction

$\theta$  : temperature dimensionless

$\lambda$  : thermal conductivity,  $W.m^{-1}.K^{-1}$   
 $\mu$  : viscosité dynamique,  $kg.m^{-1}.s^{-1}$   
 $\nu$  : dynamic viscosity,  $m^2.s^{-1}$   
 $\rho$  : density,  $kg.m^{-3}$

**Latines letters:**

A: half-width of the channel, m  
Cp: specific heat,  $J.kg^{-1}.K^{-1}$   
Da: Darcy's number  
F: Forchheimer coefficient  
Fr: Froude number  
g: gravitational acceleration,  $m.s^{-2}$   
H: thickness of the porous layer, m  
hfg: enthalpy of evaporation,  $J.kg^{-1}$   
Ja: Jacob number  
K: hydraulic conductivity or permeability,  $m^2$   
L: length of the plates of the channel, m  
Nu: local Nusselt number  
Pe: Peclet number  
Pr: Prandtl number

Re: Reynolds number  
T: temperature, K  
u: velocity along x,  $m.s^{-1}$   
 $U_0$ : velocity of the free fluid (at the entrance of the channel),  $m.s^{-1}$   
v: velocity along y,  $m.s^{-1}$   
x, y: Cartesian coordinates, m  
X: dimensionless coordinate in the longitudinal direction

**Subscripts:**

eff: effective value  
int: porous substrate / pure liquid interface  
l: liquid  
p: porous  
s: saturation  
v: steam (vapor)  
w: wall  
\*: dimensionless quantity

**References**

- [1] Shekarriz A. and Plumb O.-A, Enhancement of film condensation using porous fins, *J. Thermo physics and heat Transfer*, Vol. 3, 1989, pp. 309-314.
- [2] Chaynane R., Asbik M., Boushaba H., Zeghmami B., Khmou A. , Study of the laminar film condensation of pure and saturated vapor on the porous wall of an inclined plate. *Mechanics & Industries*, Vol. 5, No. 4, 2004, pp. 381-391
- [3] Asbik M., Chaynane R., Boushaba H., Zeghmami B. and Khmou A., Analytical investigation of forced convection film condensation on a vertical porous-layer coated surface, *Heat and Mass Transfer*, Vol. 40 (1-2) , 2003, pp. 143 – 155.  
[DOI 10.1007/s00231-002-0406-8](https://doi.org/10.1007/s00231-002-0406-8)
- [4] Momath Ndiaye, Cheikh Mbow, Joseph Sarr, Belkacem Zeghmami, Modou Faye, Numerical Investigation of Laminar Forced Thin Film Condensation of a Saturated Vapor along a Vertical Wall Covered with a Porous Material: Effect of Prandtl and Froude numbers, *International Journal on Heat and Mass Transfer Theory and Applications (IREHEAT)* , Vol. 1 N. 6, December 2013, pp 339-344.
- [5] Momath Ndiaye, Cheikh Mbow, Joseph Sarr, Belkacem Zeghmami, Numerical Study of the Thin Film-type Condensation of Saturated Forced into a Vertical Wall Covered with a Porous Material Vapor Convection. *International Journal on Heat and Mass Transfer Theory and Applications (IREHEAT)*, Vol. 1 N. 6, December 2013, pp 330-338.
- [6] Momath NDIAYE, Cheikh MBOW, Joseph SARR, Numerical Investigation of Laminar Forced Thin Film Condensation of a Saturated Vapor along a Vertical Wall

- Covered with a Porous Material, *3rd International Francophone Symposium on Energy and Mechanics, Renewable Energies and Mechanics Applied to Industry*, pp. 211-216 des Actes, 5-6-7 May 2014, Moroni (Comores) CIFEM 2014.
- [7] Momath NDIAYE, *Numerical Study of the Thin Film-type Condensation of Saturated Forced into a Vertical Wall Covered with a Porous Material Vapor Convection*, Ph.D. dissertation, Dpt of Physics, Cheikh Anta Diop University, Dakar, Senegal, 2014.
- [8] Atul A. Patil, Atul, Tejas G. Patil, Aniruddha Y. Chaudhari, Performance Evaluation of Passive Solar Water Distillation System with Separate Surface Condenser and Vacuum Pump, *International Review of Mechanical Engineering (IREME)*, Vol. 11, No 7, 467-(472) july 2017  
[10.15866/ireme.v11i7.12877](https://doi.org/10.15866/ireme.v11i7.12877)
- [9] Jha, R., Haribhakta, V., Kolte, A., Shekhadar, S., Tengale, S., Tare, S., Design and Simulation of Condensing Heat Exchanger, (2017) *International Review of Mechanical Engineering (IREME)*, vol. 11, No. 7, 2017, pp. 473-480.  
<http://dx.doi.org/10.15866/ireme.v11i7.12879>
- [10] A. Nasr, S. Al-Ghamdi, A, Numerical study of evaporation of falling liquid film on one of two vertical plates covered with a thin porous layer by free convection, *Int J Therm Sci* 112 (2017) pp.335–344.
- [11] Abdelaziz Nasr, Heat and mass transfer for liquid film condensation along a vertical channel covered with a thin porous layer, *International Journal of Thermal Sciences*, 124 (2018) 288-299.  
<http://dx.doi.org/10.1016/j.ijthermalsci.2017.10.016>
- [12] Charef A, Feddaoui M, Najim M, Meftah H. Comparative study during condensation of R152a and R134a with presence of non-condensable gas inside a vertical tube. *Heat and Mass Transfer*. 2018;54:1085-1099.  
<https://doi.org/10.1007/s00231-017-2205-2>
- [13] Mohamed El-Sayed MOSAAD and Rashed AL-AJMI, film condensation generated by free convection in a porous medium, *THERMAL SCIENCE*, Vol. 22, No. 6B, Year 2018, pp. 2699-2710. <https://doi.org/10.2298/TSCI160820316M>
- [14] Adil Charef, M'barek Feddaoui, Abderrahman Nait Alla, Monssif Najim, Computational Study of Liquid Film Condensation with the Presence of Non-Condensable Gas in a Vertical Tube, *Desalination and Water Treatment*, Chapter 4, November 5th 2018, pp.55-76.  
<http://dx.doi.org/10.5772/intechopen.76753>
- [15] Karima Sellami, Nabila Labsi, Monssif Najim, Youb Khaled Benkahla, Numerical Simulations of Heat and Mass Transfer Process of a Direct Evaporative Cooler From a Porous Layer, *Journal of Heat Transfer*, Vol. 141 / 071501, JULY 2019  
[DOI: 10.1115/1.4043302]

- [16] Ndiaye P. T., Ndiaye M., Mbow C., Ndiaye G., “Influence of Reynolds and Prandtl Numbers on Thin Film Condensation in Forced Convection in a Canal Covered with a Porous Material”. International Journal on Engineering Applications (IREA), Vol 8, n. 5, pp 178-187, September 2020. <https://doi.org/10.15866/irea.v8i5.18678>
- [17] Ndiaye P. T., Ndiaye M., Mbow C., Ndiaye G., “Numerical Study of Thin Film Condensation in Forced Convection in a Canal whose Walls Are Covered with a Porous Material: Influence of Jacob Number- Determination of Lengths of entry”. International Journal on Engineering Applications (IREA), Vol. 8, n.4, pp 125-132, July 2020. <https://doi.org/10.15866/irea.v8i4.18687>
- [18] Ndiaye P. T., Ndiaye M., Ndiaye G., Mbow C., “Numerical Study of Thin Film Condensation in Forced Convection in a Canal Whose Walls Are Covered with a Porous Material: Influence of ratio of form-Determination of Lengths of Entry”. Journal of Chemical, Biological and Physical Sciences An International Peer Review E-3 Journal of Sciences Available online at [www.jsbcs.org](http://www.jsbcs.org) Section C: Physical Sciences, JCBPS; Section C; May 2022 –July 2022, Vol. 12, No. 3; 166-180. DOI: [10.24214/jcbps.C.12.3.16680](https://doi.org/10.24214/jcbps.C.12.3.16680)
- [19] Ndiaye G., Sambou V., Ndiaye, M. and Ndiaye P.T. (2022) Numerical Study of Thin Film Condensation in Forced Convection on an Inclined Wall Covered with a Porous Material. Open Journal of Applied Sciences, 12, 793-805. <https://doi.org/10.4236/ojapps.2022.125053>
- [20] Goumbo Ndiaye, Momath Ndiaye, Vincent Sambou, Pape Tamsir Ndiaye, Madialène Sène, Cheikh Mbow. Influence of Prandtl Number on Thin Film Condensation in Forced Convection in an Inclined Wall Covered with a Porous Material. Advances in Materials Physics and Chemistry, 12, 125-140, 2022. <https://doi.org/10.4236/ampc.2022.126009>